ChemComm

Check for updates

Highly selective CO_2 electrolysis in aqueous media by a water-soluble cobalt dimethyl-bipyridine complex†

Tomiko M. Suzuki, [ID] *[a] Kengo Nagatsuka,[b] Takamasa Nonaka, [ID] [a]
Yuichi Yamaguchi, [ID] [bc] Naonari Sakamoto, [ID] [a] Takeshi Uyama, [ID] [a]
Keita Sekizawa, [ID] [a] Akihiko Kudo*[bc] and Takeshi Morikawa [ID] *[a]

A water-soluble Co complex with dimethyl-bipyridine ligands reduced CO_2 to CO electrochemically with almost 100% selectivity at -0.80 V *vs.* NHE in an aqueous medium (pH 6.8) without an organic solvent. The reaction overpotential was 270 mV. A possible CO formation mechanism was discussed based on experiments and calculations.

Reductive conversion of CO_2 into useful energy-rich chemicals using water and sustainable energy is a promising approach to ameliorating the fossil fuel shortage and mitigating global warming. Thus, the electrocatalytic CO_2 reduction reaction (CO_2RR) to form C1 chemicals such as basic ingredients carbon monoxide (CO) and formic acid is an active research topic. CO is a desirable target product because it can be converted into various hydrocarbons *via* Fischer–Tropsch synthesis. Gaseous CO exhibits low solubility in aqueous media, making its collection easier than that of liquid products such as formic acid.

Molecular metal complexes are advantageous as catalysts because their properties can be controlled through manipulation of their metal–ligand interactions; some molecular complexes therefore exhibit high reaction selectivity toward CO_2, especially in organic solvents with a sacrificial electron donor. The use of water molecules as electron donors, high CO_2 selectivity in aqueous solution, and a low overpotential for the CO_2RR are all important requirements for a sustainable catalytic system. However, CO_2 reduction by complex catalysts dissolved in almost 100% water is challenging. Nonetheless, the literature contains a few reports on selective electrocatalytic or photocatalytic CO_2RR by water-soluble metal complexes in a fully aqueous solution. Selective CO_2 reduction by water-soluble complex catalysts with macrocyclic ligands such as cyclam,

porphyrin, or their derivatives has been reported.[1–5] In addition, polypyridines such as 2,2′-bipyridine (bpy), 2,2′:6′,2″-terpyridine (tpy), and phenanthroline (phen) are common ligands in coordination chemistry and molecular catalysis because they generally construct stable, well-defined complexes. A water-soluble *fac*-[Re(CH_2OH)–OH_2]$^+$ (*fac*-[Re(4,4′-dihydroxymethyl-2,2′-bipyridine)(CO)$_3$(OH_2)]$^+$) has been reported to show electrochemical CO production with 95% selectivity at -1.1 V *vs.* normal hydrogen electrode (NHE) in an aqueous solution at pH 6.9.[6] More abundant metal elements are also desired as central metal species that drive an aqueous CO_2RR in terms of lowering the cost and reducing CO_2 emissions in the overall system lifecycle.[7–9] [Mn(bpy(COOH)$_2$)(CO)$_3$Br] (bpy(COOH)$_2$:4,4′-dicarboxy-2,2′-bipyridine) and [Cu(phen)$_2$]$^{2+}$ complexes have also been reported as water-soluble catalysts with a faradaic efficiency (FE) of 65% and $\sim$60%, respectively, for CO formation for the electrochemical CO_2RR (Table S1, ESI†).[10,11]

Water-soluble Co complexes with bpy ligands have been reported as electro- and photocatalysts for hydrogen evolution,[12] whereas their ability to function as a CO_2 reduction catalyst in aqueous solution has not yet been demonstrated. In the case of the tpy ligand, [Co(tpy)$_2$]$^{2+}$ ([Co-tpy]) has been reported to produce CO and H_2 electrochemically in a dimethyl-formamide (DMF)/H_2O (95/5 vol%) mixed solvent.[13] In the case of the bpy ligand, [Co(bpy)$_3$]$^{2+}$ ([Co-bpy] or [Co(dmbpy)$_3$]$^{2+}$ ([Co-dmbpy], dmbpy: 4,4′-dimethyl-2,2′-bipyridine) has been shown to promote the CO_2RR to produce CO and H_2 under visible-light irradiation when used in combination with a photosensitizer or a semiconductor photocatalyst in an acetonitrile (MeCN) or MeCN/H_2O mixture containing sacrificial electron donor reagents.[14–17] We recently adopted a water-soluble [Co-dmbpy] (Fig. 1a) for Z-schematic (two-step photoexcitation) photocatalysis for the CO_2RR in an aqueous suspension with two coexisting semiconductors ($BiVO_4$ for water oxidation and $(CuGa)_{0.3}Zn_{1.4}S_2$ for the CO_2RR).[18] The system demonstrated 98% CO selectivity (against 2% H_2) and 1740 µmol-CO was produced using 12 µmol [Co-dmbpy] under visible-light irradiation (wavelength $>$ 420 nm). The [Co-dmbpy] behaved as a

[a] *Toyota Central R&D Labs., Inc., 41-1 Yokomichi, Nagakute, Aichi 480-1192, Japan. E-mail: tomiko@mosk.tytlabs.co.jp, morikawa@mosk.tytlabs.co.jp*

[b] *Department of Applied Chemistry, Faculty of Science, Tokyo University of Science, 1-3 Kagurazaka, Shinjuku-ku, Tokyo 162-8601, Japan. E-mail: a-kudo@rs.tus.ac.jp*

[c] *Carbon Value Research Center, Research Institute for Science & Technology, Tokyo University of Science, 2641 Yamazaki, Noda-shi, Chiba 278-8510, Japan*

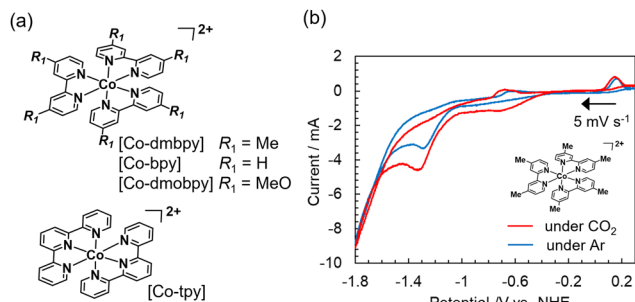† Electronic supplementary information (ESI) available. See DOI: https://doi.org/10.1039/d3cc03940d

Fig. 1 (a) Chemical structure of Co complexes with various polypyridine ligands and NO_3^- counter anions (dmbpy: 4,4'-dimethyl-2,2'-bipyridine, bpy: 2,2'-bipyridine, dmobpy: 4,4'-dimethoxy-2,2'-bipyridine, tpy: 2,2':6',2''-terpyridine). (b) CV curves for [Co-dmbpy] (0.3 mmol L^{-1}) in an aqueous $NaHCO_3$ (0.1 mol L^{-1}) solution bubbled with CO_2 (red, pH 6.8) or Ar (blue, adjusted to pH 6.8).

Fig. 2 CO_2 electrolysis of [Co-dmbpy] (0.3 mmol L^{-1}) in an aqueous $NaHCO_3$ (0.1 mol L^{-1}, 120 mL) solution at −0.85 V vs. NHE (pH 6.8) under CO_2 flow (1 atm). (a) Time-course of the total product amounts of CO and H_2 (the $HCOO^-$ content in the solution was measured at 24 h); 1/2 e^- represents the theoretical total amount of two-electron reduction products calculated from the current observed at 100% current efficiency. (b) Time-dependent rates of initial CO_2 electrolysis for gas evolution and the faradaic efficiency (FE) for CO.

redox-shuttle electron mediator for the two coexisting semi-conductors. Furthermore, experiments and calculations strongly suggested that the [Co-dmbpy] acted as a highly selective cocatalyst for CO generation by receiving electrons from $(CuGa)_{0.3}Zn_{1.4}S_2$.[18] However, the ability of the CO_2RR with unusually high selectivity over [Co-dmbpy] in an aqueous solution has not been clarified, even electrochemically.

In this communication, the electrochemical CO_2RR over the water-soluble [Co-dmbpy] was investigated. The experiments clarified that [Co-dmbpy] reduced CO_2 to CO with nearly 100% selectivity at a low potential of −0.80 V vs. NHE (pH 6.8, −0.40 V vs. reversible hydrogen electrode (RHE)), and further discussed the CO_2RR mechanism in combination with calculation.

Water-soluble divalent Co complexes [Co-R_1bpy], which have various substituents R_1 at the 2,2' position of the bpy ligand, and [Co-tpy], which has the tpy ligand (Fig. 1a), were synthesized.[18] Fig. 1b shows a current–voltage (cyclic voltammogram ⟨CV⟩) curve for [Co-dmbpy] (0.3 mmol L^{-1}) recorded in an aqueous $NaHCO_3$ (0.1 mol L^{-1}) solution bubbled with CO_2 or Ar where carbon paper (CP) and Pt wire were used as working and counter electrodes, respectively. An H-shaped two-compartment reactor separated by a Nafion membrane was used (Fig. S1, ESI†). In the CV curve under a CO_2 atmosphere (red line), a small first reduction wave from about −0.4 V vs. NHE (pH 6.8) involving a valence change of the Co ion and a larger second reduction wave from −1.0 V vs. NHE was observed. This second reduction wave is considered as the CO_2 reduction current over the complex. On the other hand, the Ar atmosphere (blue line, in the absence of CO_2) shows a similar CV curve, but the current values for the two reduction waves are lower than for the CO_2 atmosphere, especially the first reduction wave, which yields very small current. We focused on this first reductive peak and performed CO_2 electrolysis at −0.85 V vs. NHE for 24 h. A continuous reaction current of around −0.26 mA was generated (Fig. S3, ESI†). Fig. 2 shows the time-courses of the reduction products and faradaic efficiency (FE) for CO over [Co-dmbpy]. CO was predominantly produced, with trace amounts of H_2 and formic acid, whereas other gaseous species such as methane were not detected. The
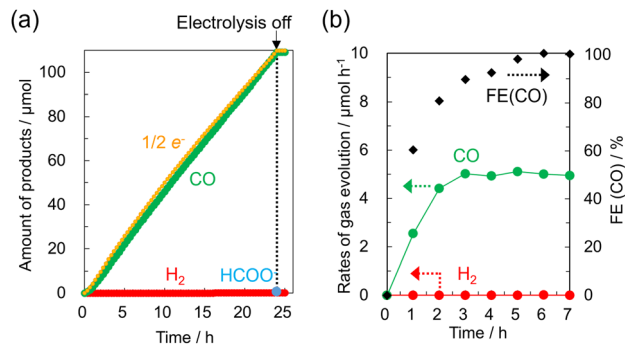
CO generation rate stabilized at a value of ∼5 μmol h^{-1} after the induction period for 3 h, with the FE for CO formation reaching almost 100% after 5 h of electrolysis (Fig. 2b). As shown in Fig. 2a, the amount of CO (green) produced increased almost linearly, approximately consistent with the ideal value calculated from the number of electrons measured (orange) for the two-electron reduction reaction. The CO selectivity among the total reduction products (CO, H_2, and $HCOO^-$) in 24 h reached 99.8%. The turnover number was 3.0, suggesting that this CO_2RR was catalytic. When electrolysis was terminated, the formation of gas-phase components quickly ceased. These results show that a stable and highly CO_2-selective catalyst originated from [Co-dmbpy] after a certain induction time. No reduction products were detected in electrolysis under the same conditions (−0.85 V vs. NHE, pH 6.8) in an Ar atmosphere (Fig. S4, ESI†), suggesting that CO formation is due to CO_2 reduction. In the UV-Vis spectrum of the CO_2 electrolysis solution, the peaks originating from π–π* transitions of the Co complex showed almost no change between before and after 24 h of electrolysis, suggesting that the Co component was still present as a water-soluble complex in the solution even after the CO_2RR (Fig. S5, ESI†). No evidence originating from hetero-geneous species of Co components was detected on the CP electrode after 24 h of electrolysis, suggesting that the homo-geneous species in the solution were driven as catalysts (Fig. S6 and S7, ESI†). From CO_2 electrolysis at different potentials, the overpotential for CO generation was estimated to be 270 mV relative to the theoretical value[19,20] (Table S1, entry 1 and Fig. S8, ESI†). Thus, [Co-dmbpy] achieved greater CO selectivity at lower potentials during CO_2 electrolysis than previously reported water-soluble molecular catalysts with polypyridine ligands (Table S2, ESI†). The CO selectivity varied significantly with the applied potential. For example, in the CO_2 electrolysis at −1.3 V vs. NHE (at pH 6.8), near the second reductive peak in the CV, competitive H_2 production was more predominant than CO production (Table S1, entry 4 and Fig. S9, ESI†). This result indicates that the CO_2RR proceeds at a more positive potential

than that for H_2 production over [Co-dmbpy], despite the reaction occurring in an aqueous medium, as shown in the CV curves acquired under Ar and CO_2 (Fig. 1b).

To measure the change in the electronic state of Co in the aqueous solution at the cathode side, we carried out *operando* X-ray absorption spectroscopy (XAS) measurements *via* a fluorescence detection method (Fig. S2, ESI†). XAS measurements of Co complexes in such a dilute (0.5 mmol L^{-1}) aqueous solution have not been reported. As shown in the Co K-edge X-ray absorption near edge structure (XANES) spectra originated from [Co-dmbpy] in Fig. 3a, immediately after a potential was applied (as an integrated signal for 0–20 min), the energy position of half-value of the normalized absorbance of the Co K-edge energy shifted negatively by 1.5 eV and the profile was stabilized even after electrolysis for 3 h. Another *operando* setup that allowed ~90% of Co K-edge X-ray signal to be attributed to the CP vicinity also yielded an XANES peak shift similar to that in Fig. 3a (Fig. S10 and S11, ESI†). These significant shifts are due to electron injection into Co complexes at −0.85 V *vs.* NHE, which might accompany a structural change to an active catalyst. Fig. 3b shows the proposed mechanism for estimating the electrochemical CO_2RR by [Co-dmbpy] based on the density functional theory (DFT) calculations. The calculations suggested that a ligand-decoordinated species of $[Co(dmbpy)_2]^{2+}$(**1**) is formed as an active monomer catalyst by the decoordination of one dmbpy

ligand in [Co-dmbpy]. The energy diagram results based on the calculations for the two-coordinated complex (Fig. S12, ESI†) indicate that the highest energy barrier in the scheme of Fig. 3b is the process from **2** → **3** (CO_2 coordination), which is the rate-limiting step in the overall CO_2RR. Therefore, it is considered that the −1.5 eV shift in the *operando* XANES spectra is attributable mainly to the active species **2**.

To verify the above hypothesis, we synthesized a pseudo-two-coordinate complex by mixing Co^{2+} and twice the amount (equivalent) of dmbpy (hereafter, [Co/dmbpy = 1/2]), and we performed CO_2 electrolysis using it as a catalyst (Fig. S13–S15, ESI†). The induction period for CO formation by [Co/dmbpy = 1/2] was reduced to less than half that for the three-coordinated [Co-dmbpy] (Fig. S15, ESI†). These results suggest that the active species could be the two-coordinated species and the three-coordinated species is most likely a pre-catalyst.

Table 1 summarizes the results of the electrochemical CO_2RR for three types of Co complexes having bpy-based ligands with different electron-donating substituents, [Co-tpy], and Co^{2+} ions but without any ligands, as measured at −0.85 V *vs.* NHE for 6 h in $NaHCO_3$ aqueous solution (the corresponding structures are shown in Fig. 1a). First, in the case of an aqueous $NaHCO_3$ solution with no Co components, the generation rates for CO and H_2 at 6 h were very low: 0.54 and 0.28 μmol h^{-1}, respectively (entry 8). These low rates were attributed to the reaction at the bare CP electrode as previously reported.[11] Only hydrogen was produced by Co^{2+} ions without ligands preferred for CO_2 adduct formation (entry 7), indicating that the Co complexes function as a CO_2RR catalyst. By contrast, the [Co-dmbpy] produced CO and H_2 rates of 5.13 and 0.01 μmol h^{-1}, respectively, along with a small amount (0.1 μmol) of $HCOO^-$; the selectivity toward CO among the total amount of products reached 99.6%, and the catalyst even suppressed H_2 generation at the carbon substrate (entry 1). [Co-bpy] and [Co-dmobpy] (dmobpy: 4,4-dimethoxy-2,2-bipyridine) produced CO at rates of 2.01 and 3.72 μmol h^{-1} with CO
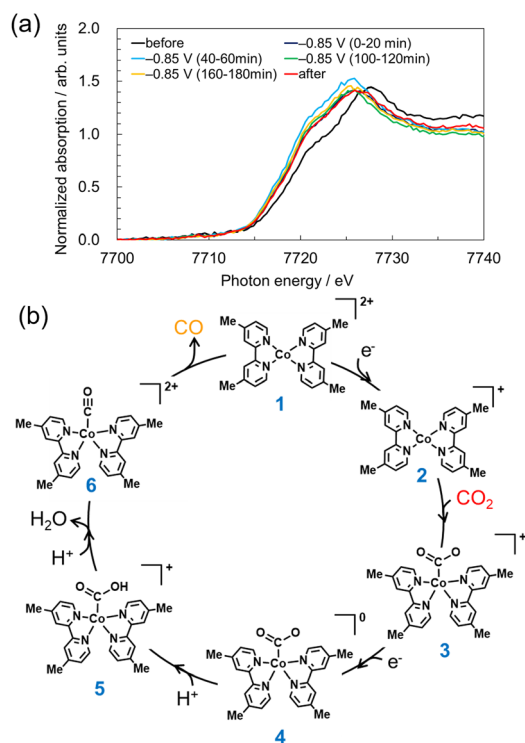

Fig. 3 (a) *Operando* Co K-edge XANES spectra of 0.5 mmol L^{-1} [Co-dmbpy] measured at open circuit (OC) voltage (before: black), CO_2 electrolysis (−0.85 V *vs.* NHE at pH 6.8), and after the electrolysis measured at OC voltage (after: red) measured in an aqueous 0.1 mol L^{-1} $NaHCO_3$ solution bubbled with CO_2. (b) Proposed electrocatalytic reduction mechanism for CO_2 to CO by two-coordinated complex **1** in an aqueous solution based on DFT calculation.

Table 1 CO_2 electrolysis of 0.3 mmol L^{-1} Co compound in an aqueous $NaHCO_3$ solution at −0.85 V (*vs.* NHE at pH 6.8) for 6 h[a]

Entry	Co compound	Current, 6 h/mA	Rate of products, 6 h/μmol h^{-1}		CO selectivity/%[b]
			CO	H_2	
1	[Co-dmbpy]	−0.26	5.13	0.01	99.6
2	[Co-tpy]	−0.16	0.73	0.52	57.2
3	[Co-bpy]	−0.12	2.01	0.19	86.8
4	[Co-dmobpy]	−0.21	3.72	0.11	95.8
5	$[Co(bpy)_3]Cl_2$[c]	−0.11	1.64	0.14	87.1
6	$[Co(bpy)_3]Cl_3$[d]	−0.11	1.43	0.16	92.6
7	$Co(NO_3)_2$	−0.92	0.00	20.2	0.0
8	None	−0.055	0.54	0.28	65.9

[a] Carbon paper, Ag/AgCl, and Pt wire were used as working, reference, and counter electrodes, respectively. The pH of the 0.3 mmol L^{-1} Co compound/aqueous $NaHCO_3$ (0.1 mol L^{-1}) solution under CO_2 (1 atm) was approximately 6.8. Electrolysis was performed for 6 h, and the production rate at 6 h is shown. [b] Calculated from the rate of CO generation in relation to the total amount of reduced products (CO, H_2, and $HCOO^-$) for 6 h. [c] Commercial product; $[Co(II)(bpy)_3]Cl_2 \cdot 5H_2O$. [d] Commercial product; $[Co(III)(bpy)_3]Cl_3 \cdot 4H_2O$.

selectivities of 86.8% and 95.8%, respectively (entries 3 and 4). Commercially available complexes [Co(II)-bpy] and [Co(III)-bpy] with Cl⁻ as the counter ion (entries 5 and 6) also exhibited activities similar to that for the synthesized [Co(II)-bpy] with NO_3^- as the counter ion (entry 3). In particular, [Co-dmbpy] and [Co-dmobpy] with electron-donating ligands on bpy yielded high CO selectivity greater than 95%. This result is consistent with the results of the DFT calculations: the electron-donating groups increase the electron density at the Co center, resulting in stronger bonding with CO_2 and promoting the CO_2RR.[18] In the case of [Co-tpy], the rate of CO generation was 0.73 μmol h⁻¹ and the CO selectivity was 57.2%, which was inferior to the performance of Co complexes with bpy-based ligands (entry 2). This result is consistent with the observation that the Z-schematic CO_2RR rate using the [Co-tpy] was low in a previous study.[21] [Co-tpy] might require much more negative potential to activate by decoordination of a tpy ligand, as suggested in a previous study that included an experiment conducted in DMF–H_2O containing tetrabutylammonium perchlorate (TBAP) electrolyte.[13]

We here discuss the reason why CO_2 electrolysis of an aqueous Co complex solution occurred even at a low potential equivalent to −0.80 V vs. NHE. With respect to the mechanism of the lowered CO_2RR potential over the Co porphyrin, DFT calculations suggest that water facilitated CO_2 reduction through a concerted pathway involving a hydrated metal complex.[22] DFT calculations and experiments have revealed that a reaction at the Mn-bpy, in harmony with metal cations and the carbon substrate, changes the CO_2RR from an endothermic to an exothermic reaction.[8,23] In Re complexes, a mechanism due to dimerization has been proposed for the formation of CO in CO_2 reduction at high potential regions based on the one-electron pathway, which may also be the case in this system, but it is not evident.[6] Further detailed mechanistic analyses are important, and progress based on the investigations is expected for the present water-soluble [Co-dmbpy] system operating at the low potential regions.

The present [Co-dmbpy] yields CO with nearly 100% selectivity at a low potential of −0.80 V vs. NHE (pH 6.8). In the Z-schematic CO_2RR photocatalysis, [Co-dmbpy] was coupled with the $(CuGa)_{0.3}Zn_{1.4}S_2$ semiconductor to produce CO with 98% selectivity under visible-light irradiation.[18] The conduction-band minimum (CBM) of $(CuGa)_{0.3}Zn_{1.4}S_2$ is located at a substantially more negative position (−1.66 V vs. NHE at pH 5.9). In a femtosecond transient spectroscopy study of a hybrid photocatalyst composed of an N-doped Ta_2O_5 (N-Ta_2O_5) semiconductor linked with a Ru complex having bpy ligands [Ru-bpy], electron injection to the [Ru-bpy] not only from the CBM but also via shallow traps of the N-Ta_2O_5 semiconductor was confirmed.[24] Thus, electron injection from shallow traps of $(CuGa)_{0.3}Zn_{1.4}S_2$ to the two-coordinate Co complex is also expected to produce CO (Fig. S16, ESI†). Because of the low overpotential for the CO_2RR over the [Co-dmbpy] complex, sufficient room exists to apply it to various semiconductors to construct an efficient photosystem.[20,25] This possibility warrants further study in the near future.

In summary, a water-soluble Co(II) complex with dimethyl-bipyridine ligands functioned as an unparalleled electrocatalyst to drive the CO_2RR in an aqueous hydrogen carbonate solution

bubbled with CO_2. CO_2 reduction to CO occurred at a low potential of −0.80 V vs. NHE (pH 6.8) with a CO selectivity approaching 100%. Because the activity emerges in an aqueous solution without any organic solvents, it is beneficial to CO_2 reduction setups that use water as an electron donor in electrocatalysis and photocatalysis.

Conflicts of interest

There are no conflicts to declare.

Notes and references

1 M. Beley, J. P. Collin, R. Ruppert and J. P. Sauvage, J. Am. Chem. Soc., 1986, 108, 7461–7467.
2 C. Costentin, M. Robert, J. M. Saveant and A. Tatin, Proc. Natl. Acad. Sci. U. S. A., 2015, 112, 6882–6886.
3 A. Call, M. Cibian, K. Yamamoto, T. Nakazono, K. Yamauchi and K. Sakai, ACS Catal., 2019, 9, 4867–4874.
4 Q.-Q. Bi, J.-W. Wang, J.-X. Lv, J. Wang, W. Zhang and T.-B. Lu, ACS Catal., 2018, 8, 11815–11821.
5 K. E. Dalle, J. Warnan, J. J. Leung, B. Reuillard, I. S. Karmel and E. Reisner, Chem. Rev., 2019, 119, 2752–2875.
6 A. Nakada and O. Ishitani, ACS Catal., 2018, 8, 354–363.
7 H. Takeda, C. Cometto, O. Ishitani and M. Robert, ACS Catal., 2017, 7, 70–88.
8 S. Sato, K. Saita, K. Sekizawa, S. Maeda and T. Morikawa, ACS Catal., 2018, 8, 4452–4458.
9 M. Wang, K. Torbensen, D. Salvatore, S. Ren, D. Joulié, F. Dumoulin, D. Mendoza, B. Lassalle-Kaiser, U. Işci, C. P. Berlinguette and M. Robert, Nat. Commun., 2019, 10, 3602.
10 J. J. Walsh, G. Neri, C. L. Smith and A. J. Cowan, Organometallics, 2018, 38, 1224–1229.
11 J. Wang, L. Gan, Q. Zhang, V. Reddu, Y. Peng, Z. Liu, X. Xia, C. Wang and X. Wang, Adv. Energy Mat., 2019, 9, 1803151.
12 S. P. Luo, L. Z. Tang and S. Z. Zhan, Inorg. Chem. Commun., 2017, 86, 276–280.
13 N. Elgrishi, M. B. Chambers, V. Artero and M. Fontecave, Phys. Chem. Chem. Phys., 2014, 16, 13635–13644.
14 Y. Yao, Y. Gao, L. Ye, H. Chen and L. Sun, J. Energy Chem., 2018, 27, 502–506.
15 J. Lin, Z. Pan and X. Wang, ACS Sustainable Chem. Eng., 2013, 2, 353–358.
16 J. J. Walsh, C. Jiang, J. Tang and A. J. Cowan, PCCP, 2016, 18, 24825–24829.
17 Y. Zhang, M. Cao, H. Feng, D. Liu and Q. Li, ACS Catal., 2023, 13, 11376–11388.
18 T. M. Suzuki, S. Yoshino, K. Sekizawa, Y. Yamaguchi, A. Kudo and T. Morikawa, Appl. Catal., B, 2022, 316, 121600.
19 S. Yoshino, T. Takayama, Y. Yamaguchi, A. Iwase and A. Kudo, Acc. Chem. Res., 2022, 55, 966–977.
20 H. N. Tian, ChemSusChem, 2015, 8, 3746–3759.
21 T. M. Suzuki, S. Yoshino, T. Takayama, A. Iwase, A. Kudo and T. Morikawa, Chem. Commun., 2018, 54, 10199–10202.
22 K. Miyamoto and R. Asahi, J. Phys. Chem. C, 2019, 123, 9944–9948.
23 T. Morikawa, S. Sato, K. Sekizawa, T. M. Suzuki and T. Arai, Acc. Chem. Res., 2022, 55, 933–943.
24 K. Yamanaka, S. Sato, M. Iwaki, T. Kajino and T. Morikawa, J. Phys. Chem. C, 2011, 115, 18348–18353.
25 H. Kumagai, G. Sahara, K. Maeda, M. Higashi, R. Abe and O. Ishitani, Chem. Sci., 2017, 8, 4242–4249.